

Soft γ -ray selected radio galaxies: favouring giant size discovery

L. Bassani,^{1*} T. Venturi², M. Molina¹, A. Malizia¹, D. Dallacasa^{3,2},
F. Panessa⁴, A. Bazzano⁴, P. Ubertini⁴

¹ INAF/IASF Bologna, Via P. Gobetti 101, I-40129 Bologna, Italy

² INAF/IRA Bologna, Via P. Gobetti 101, I-40129 Bologna, Italy

³ Dipartimento di Fisica e Astronomia, Università di Bologna, Via Ranzani 1, 40127, Bologna, Italy

⁴ INAF/IAPS Roma, Via Fosso del Cavaliere 100, I00133 Rome, Italy

ABSTRACT

Using the recent INTEGRAL/IBIS and Swift/BAT surveys we have extracted a sample of 64 confirmed plus 3 candidate radio galaxies selected in the soft gamma-ray band. The sample covers all optical classes and is dominated by objects showing a FR II radio morphology; a large fraction (70%) of the sample is made of “radiative mode” or High Excitation Radio Galaxies (HERG). We have measured the source size on NVSS, FIRST and SUMSS images and have compared our findings with data in the literature obtaining a good match. We surprisingly found that the soft gamma-ray selection favours the detection of large size radio galaxies: 60% of objects in the sample have size greater than 0.4 Mpc while around 22% reach dimension above 0.7 Mpc at which point they are classified as Giant Radio Galaxies or GRGs, the largest and most energetic single entities in the Universe. Their fraction among soft gamma ray selected radio galaxies is significantly larger than typically found in radio surveys, where only a few percent of objects (1-6%) are GRGs. This may partly be due to observational biases affecting radio surveys more than soft gamma ray surveys, thus disfavouring the detection of GRGs at lower frequencies. The main reasons and/or conditions leading to the formation of these large radio structures are still unclear with many parameters such as high jet power, long activity time and surrounding environment all playing a role; the first two may be linked to the type of AGN discussed in this work and partly explain the high fraction of GRGs found in the present sample. Our result suggests that high energy surveys may be a more efficient way than radio surveys to find these peculiar objects.

Key words: Galaxies – AGN – gamma-rays – Radio.

1 INTRODUCTION

A small fraction of radio galaxies (around 6% in the 3CR catalogue, Ishwara-Chandra & Saikia, 1999) exhibits extraordinary linear extents, i.e. above 0.7 Mpc (for $H_0 = 71 \text{ km s}^{-1} \text{ Mpc}^{-1}$, $\Omega = 0.27, \Omega_\Lambda = 0.73$). Defined as Giant Radio Galaxies (GRGs), these objects represent the largest and most energetic single entities in the Universe and are of particular interest as extreme examples of radio source development and evolution; indeed they are the ideal targets to study the duty cycle of radio activity. Furthermore, it has been proposed that they can play a role in the formation of large-scale structures and can be used to probe the Warm-Hot Intergalactic Medium (Malarecki et al 2013). In addition, GRGs are unique laboratories to study particle acceleration processes and understand cosmic magnetism (Kronberg et al. 2004).

GRGs are difficult to discover for two main reasons: a) the low surface brightness of their extended emission requires sensitive radio telescopes to be detected and b) they are often composed

of bright knots spread over a large area which are difficult to associate to a single radio source. As a result, only around 300 GRGs are known to date (Wezgowiec, Jamrozny and Mack 2016 and references therein).

Both Fanaroff-Riley type I and type II radio galaxies (FRI and FRII respectively, Fanaroff & Riley, 1974) are represented in samples of GRGs. While FRI giant radio galaxies are associated with early type galaxies, those with FRII morphology are hosted both in early type galaxies and quasars. Lara et al. (2001 and 2004) studied the statistical properties of a sample of GRGs selected from the NRAO VLA Sky Survey (NVSS) and found roughly the same fraction of FRI and FRII sources, the FRIIs being at much higher redshifts mainly due to the fact that they have higher power and are edge brightened. The samples of GRGs available in the literature, mainly drawn from radio surveys such as the NVSS, the Sydney University Molonglo Sky Survey (SUMSS) and the Westerbork Northern Sky Survey (WENSS) (Cotter et al. 1996; Lara et al. 2001; Machalski et al. 2001; Machalski et al. 2006; Saripalli et al., 2005; Schoenmakers et al. 2001), have been used to test models of radio galaxy evolution (e.g. Blundell et al. 1999). On the basis of

* E-mail address: bassani@iasfbo.inaf.it

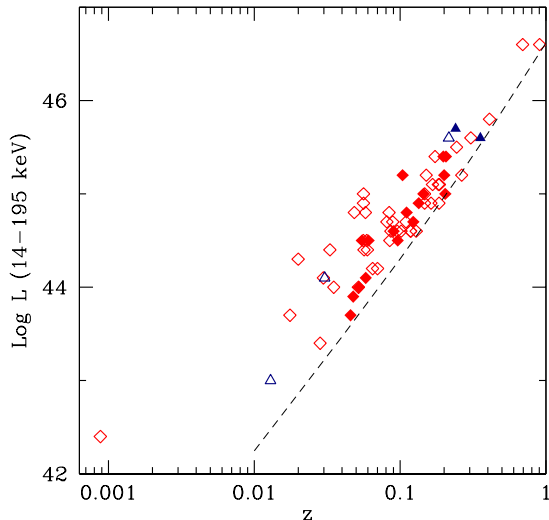


Figure 1. Soft gamma-ray luminosity (14-195 keV) vs redshift for the whole sample. Diamonds are BAT luminosity values while triangles are IBIS ones converted to the proper waveband using a power law fit to the INTEGRAL spectrum; filled symbols represent giant radio galaxies. The dashed line represents the sample limiting flux at around 9×10^{-12} ergs $\text{cm}^{-2} \text{s}^{-1}$.

the assumption that spectral ages of radio galaxies are representative of their intrinsic ages (Parma et al. 1999)¹, GRGs are found to be on average old sources with measured radiative ages in excess of 10^8 yr.

Beyond the source age, the main intrinsic parameters which allow a radio galaxy to reach a linear size of the order of the Mpc during its lifetime are still unclear. The role of the external medium is difficult to evaluate, not to mention that the density of the medium surrounding the jets and lobes may change considerably over the large scales considered here. Some GRGs are associated with the dominant member of a galaxy group (as is the case for instance of the FRI GRG NGC315, Giacintucci et al. 2011), while others have been detected at high redshift in a likely less dense environment. This has been confirmed more quantitatively by Machalski et al. (2004), in a comparative study of GRGs and normal sized radio galaxies. They concluded that the jet power and the central galaxy density seem to correlate with the size of radio galaxies. All in all, however, the origin and evolution of GRGs remains unclear. In this paper we argue that soft gamma-ray surveys provide a different way to discover and study these intriguing objects and give therefore a new perspective into their nature and origin.

2 THE SAMPLE

The extent of the emission in radio-loud AGN ranges from less than 100 kpc up to a few Mpc and so a first step to uncover extended radio galaxies is to study the radio morphology of well defined sam-

ples of AGN. In this work we concentrate on two samples of active galaxies selected in the soft gamma-ray band. This waveband provides a very efficient way to find nearby AGN since it is transparent to obscured regions/objects, i.e. those that could be missed at other frequencies such as optical, UV, and even X-rays. This waveband favours the discovery of “radiative mode” objects, one of the two main flavours of the AGN radio population (see Heckman and Best 2014 for a review of each population properties). The alternative name for these sources, high ionization or high excitation AGN, is related to the level of ionization of the Narrow Line Region gas. In the “radiative mode” AGN, accretion is postulated to occur via a radiatively efficient accretion disc (e.g. Shakura & Sunyaev 1973). The current soft gamma-ray instrumentation tends to uncover the brightest active galaxies in the sky and hence to favour the discovery of accretion dominated AGN, also among radio galaxies.

Since 2002, the soft gamma-ray sky is being surveyed by INTEGRAL/IBIS and subsequently by Swift/BAT at energies greater than 10 keV; up to now various all sky catalogues have been released, based on the data collected by these two satellites (see for example Bird et al. 2010 and Baumgartner et al. 2013). These catalogues contain large fractions of active galaxies, i.e. $\sim 30\%$ among INTEGRAL/IBIS and up to 70% among Swift/BAT sources. For the purpose of this work we use one sample extracted from INTEGRAL/IBIS and one from Swift/BAT data; together these two samples provide the most extensive list of soft gamma-ray selected active galaxies known to date. For INTEGRAL, we consider the sample of 272 AGN discussed by Malizia et al. (2012) added with four sources that have been discovered or identified with active galaxies afterwards (Landi et al. 2010, Masetti et al. 2013, Krivonos et al. 2012). For Swift/BAT we use the 70 month catalogue of Baumgartner et al. (2013) which lists 822 objects associated with AGN or galaxies; in this case we also consider the sample of 65 unknown objects in an attempt to uncover all possible radio galaxies in the BAT sample.

Then we searched for radio counterparts using the NVSS (Condon et al. 1998), the FIRST (White et al. 1997) and the SUMSS (Mauch et al. 2003). All together we inspected around 1000 images to uncover those sources that are extended (with lobes and jets) on radio maps and therefore display a double lobe morphology typical of radio galaxies. For each radio galaxy we measured the largest angular size (LAS) in arcsec and then calculated the corresponding projected linear size in Mpc at the source redshift assuming the standard cosmological parameters ($H_0 = 71 \text{ km s}^{-1} \text{ Mpc}^{-1}$, $\Omega = 0.27$, $\Omega_\Lambda = 0.73$). For all objects located north of declination -40° we used NVSS maps, the accuracy of which is $\sim 10''$, i.e. 1/4 of the angular resolution. We also complemented such information with images at 1.4 GHz from the FIRST survey whose smaller point spread function or PSF ($5''$ against $45''$ of the NVSS) allows better accuracy (of the order of $1.5''$). Nine objects south of $\delta = -40^\circ$ were searched for in the SUMSS survey, and similarly measured. Here the accuracy is worse, $\sim 20''$, as a result of a wider PSF. For most objects the LAS value obtained in this way is in quite good agreement with literature information. In a few cases there is some discrepancy, mainly arising from artifacts in the image (e.g. 3C 84 and both Centaurus A and Centaurus B) and/or complex radio structure/environment (e.g. 3C 84 and 3C 120); when relevant, notes are reported in Table 2. Considering that our sample spans a broad range of redshifts, from the local Universe (e.g. 3C 84 at $z=0.017559$) to intermediate distances, such as the case of 3C 309.1 ($z=0.905$), the uncertainty in the linear size estimate is not constant in our sample. Conversion factors between the angular and linear

¹ Note that spectral ages are systematically lower than dynamical ages and it is still unclear which best represents a source intrinsic age (Harwood, Hardcastle and Croston 2015 and references therein)

scale are given in Table 2 and can be used to estimate the uncertainty on each measurement.

All the information gathered has been summarised in Table 2 where for each source, we list redshift, optical class, radio morphology, soft gamma-ray luminosities as measured by INTEGRAL/IBIS in the 20-100 keV band and/or Swift/BAT in the 14-195 keV band and data on the radio size. In particular we quote the conversion from arcsec to kpc, the radio size (in arcsec and Mpc) as reported in the literature with relative reference and the radio size (in arcsec and Mpc) measured by us in this work. Soft gamma-ray luminosities have been estimated from our own INTEGRAL/IBIS spectra (but see also Malizia et al. 2012 for flux values) or have been taken from Baumgartner et al. (2013) for SWIFT/BAT objects.

3 RESULTS

3.1 Sample characteristics

All together we uncovered 64 radio galaxies with a double lobe morphology plus 3 objects which display a less clear radio structure and are therefore candidate radio galaxies. PKS 0921–213 and 2MASX J23272195+1524375 seem to be associated to radio emission made by several components that could belong to a single radio source; the fact that there are no optical objects at the center of their putative radio lobes is positive but sensitive radio continuum images with lower spatial resolution are necessary to confirm the double lobe morphology of both objects. IGR J18249–3243 is instead unresolved on the NVSS map; it is both the most distant source in the INTEGRAL/IBIS complete sample of AGN discussed by Panessa et al. (2015) and the most extended one. Also in this case better imaging is necessary to confirm the double lobe morphology. Interestingly all 3 candidates have a large radio size, with 2 objects displaying an extent close to 1 Mpc and this is the main reason why we kept them in the sample although as cases to be confirmed. 27 objects are from the INTEGRAL survey, 62 from the Swift survey, 22 have a detection in both. The fraction of double lobe radio galaxies which are present in soft gamma-ray catalogues of AGN was found to be around 7% (64/887) for Swift/BAT and 10% (27/274) for INTEGRAL/IBIS. Only 2 sources are still optically unclassified: one does not have redshift information while the other has a photometric z value.

Figure 1 is a plot of the soft gamma-ray (14-195 keV) luminosity versus redshift for the whole sample² As shown in figure 1 the sample flux limit is around 9×10^{-12} ergs cm^{-2} s^{-1} . The redshift values span from 0.0008 to 0.905 with a mean at 0.136 while the luminosities range from $\text{Log}(L_{14-195\text{keV}})=42.4$ ergs s^{-1} to $\text{Log}(L_{14-195\text{keV}})=46.6$ ergs s^{-1} with a mean at $\text{Log}(L_{14-195\text{keV}})=44.7$ ergs s^{-1} ; these luminosities are quite high, intermediate between Seyfert and Blazar values (see for comparison Malizia et al. 2012 and Baumgartner et al. 2013).

As summarized in Table 1, the sample contains AGN of various optical classes and, as expected, it is dominated by FR II objects since high excitation AGN (both of type I and II) are generally associated to this type of radio morphology (Buttiglione et al. 2009.

Table 1. Sample classification

Opt Class	Morph Type
25 type 1	51 FR II [†]
12 type 1.2-1.5	6 FR I [†]
9 type 1.8-1.9	6 FR I/FR II
19 type 2	1 C
2 Unknown	3 unknown

[†] Including also uncertain types

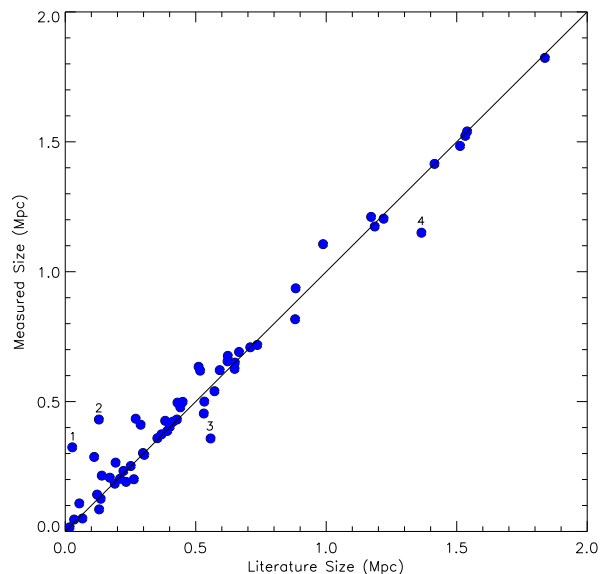


Figure 2. Measured versus literature size both in Mpc. Straight line represents the 1-1 correspondence between sizes. Numbers corresponds to some sources with notes in Table 2: 1=3C084/NGC1275, 2=PKS 1916-300, 3=3C120, 4=B3 0309+411B

We point out that the reverse is not true. Using the observed luminosities, the bolometric correction adopted by Mushotzky et al. (2008) for BAT AGN and by Molina et al. (2014) for IBIS AGN³ and typical black hole masses in the range 10^7 - 10^9 solar masses, we estimate Eddington ratios ranging from 0.001 up to 0.1, which suggests that all our objects are indeed efficiently accreting, or “radiative mode” AGN. To confirm this initial indication, we have also checked the literature to find information regarding the excitation mode of the narrow line region gas in the host galaxy of each source. We find that around 70% of the sources can be defined as high excitation objects according to various studies in the literature (Gendre et al. 2013, Buttiglione et al 2010, Landt et al. 2010, Hardcastle et al. 2009, Winter et al. 2010, Schoenmakers et al 1998, Lewis et al. 2003), while the remaining 30% have no data for an unambiguous classification.

3.2 Radio extent of sample objects

Table 2 reports the largest linear size of the radio galaxies in the sample (Sect. 2). For completeness in Column 8 we also report

² BAT luminosities have been preferred for this plot as they cover more sources; IBIS 20-100 keV luminosities for 5 objects not detected by BAT have been converted to 14-195 KeV luminosities using best fit spectral parameters.

³ $L_{\text{bol}} = 15 L_{\text{BAT}}$ and $L_{\text{bol}} = 25 L_{\text{IBIS}}$

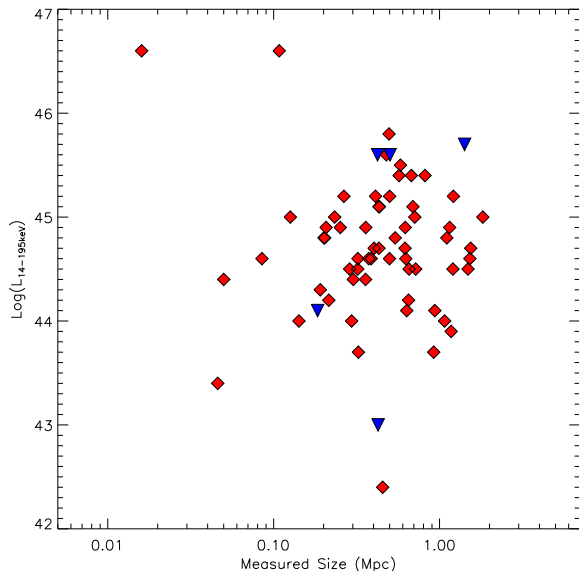


Figure 3. Soft gamma-ray luminosity (14-195 keV) versus measured size; red diamonds are BAT luminosity values while blue triangles are IBIS ones converted to the proper waveband using a power law fit to the INTEGRAL spectrum.

literature values, based on individual studies. The comparison between the two values is shown in Fig. 2. We point out that the values found in the literature are very inhomogeneous, as they refer to interferometric radio observations whose resolution and frequency is very different from the 0.843-1.4 GHz NVSS/FIRST/SUMSS images, hence it is not surprising that we see some differences. Our measurements are affected by some uncertainties, as described in the previous section, but in any case considering the purpose of the present paper, i.e. estimate the fraction of giant radio galaxies in our sample, the difference in size is in all cases irrelevant.

Therefore, considering the good match between our sizes and those reported in the literature and the fact that our estimates cover the entire sample, while literature information are lacking for some sources, for the following discussion we will adopt the values reported in the last column of Table 2, i.e. our own measurements, keeping in mind the uncertainties given on the source size and the mismatch found for some sources.

The size distribution of the radio galaxies in the sample shows an almost continuous coverage, from ~ 20 kpc (3C 390.1) up to ~ 2 Mpc (2MASXJ14364961-1613410), with many sources displaying LAS values above few hundred kpc: indeed 60% of the objects in the sample have sizes above 0.4 Mpc. If we consider the classical threshold to define a giant radio galaxy out of the 67 radio galaxies in this work, we find 16 objects with size ≥ 0.7 Mpc, i.e. 24% of the total. Even if we keep a more conservative approach and remove all candidate objects, we still find 14 giant radio galaxies; this represents 22% of the sample. Taking into account that a couple of sources (i.e. 3C 206 and 4C+18.51) have dimension close to 0.7 Mpc, this fraction should be considered as a lower limit.

GRGs are very rare objects in the AGN radio loud population. For instance, in the 3CR catalogue of radio galaxies only 6% are giant (Ishwara-Chandra & Saikia 1999), and if we restrict to the Local Universe ($z \leq 0.2$) their fraction decreases to 1% (Andernach et al. 2014). Such small fraction can be interpreted as due to a number of observational biases, which severely affect their inclusion

in large samples. The most relevant are the Malmquist bias, which disfavors the detection of faint sources at high redshift, and the linear size bias, which tends to bias high redshift samples in favour of radio galaxies with very large linear size. i.e. only the peak of the iceberg. At low redshift GRGs are disfavoured both as consequence of the small volume sampled, and of the fact that very diffuse radio lobes may be resolved out by interferometric observations, not to mention that the radio lobes typically have a very steep spectrum, which makes their detection challenging at frequencies above a GHz. Indeed the fraction of giant radio galaxies is expected to increase in the new low frequency surveys such as MSSS (LOW Frequency ARray, LOFAR) and GLEAM (Murchison Widefield Array, MWA). Soft gamma-ray surveys are not affected by these biases, which may explain the considerably higher fraction we report in this paper.

4 PRELIMINARY CONSIDERATIONS

Apart from the selection effects describe above, it is also possible that the difference in the fraction of GRGs found between radio and soft gamma-ray surveys is due to biases related to the sample selection. Our sample is dominated by HERGs of the FRII type: these are probably among the most powerful objects of the FRII population (Saripalli 2012) and could well be those more capable of producing giant structures. If we consider the sample of FRII radio galaxies discussed by Nilsson (1998), take the radio size of only those objects with redshift and assume the same cosmology adopted in this work, we find that out of 672 objects listed in that work 38 (or 5.6%) qualify to be radio giants. Similarly using the 401 FR II galaxies in the SDSS sample discussed by Koziel-Wierzbowska and Stasinska (2011) we find that 22 objects have size above 0.7 Mpc, i.e. 5.5% of the sample. These percentages are very similar to the one reported for the 3CR sample by Ishwara-Chandra & Saikia (1999). However, both selections do not distinguish between low and high excitation objects: if this is done for example considering the sample of Buttiglione et al (2010) where each source is well classified in terms of the relative intensity of low and high excitation lines, out of 46 high excitation objects with a reported redshift only 1 is giant (or 2% of the sample). Thus the radio morphology of the objects discussed in this work does not seem to provide a bias towards the selection of giant radio galaxies.

On the other hand our objects are among the brightest and most powerful AGN in the sky, their soft gamma-ray luminosities are just below those of powerful blazars and their Eddington ratios indicate quite efficient accretors. This immediately suggests that these soft gamma-ray selected radio galaxies have central engines powerful enough to produce large scale radio structures: a large fraction of the objects in the sample have sizes above few hundred Kpc and more than 20% reach giant dimensions. If the soft gamma-ray luminosity is a measure of the source power then one should expect a correlation between this parameter and the source radio size. However no such correlation is evident in the plot of these two quantities shown in figure 3.

The analytical models describing the evolution of radio galaxies (see for example Kaiser and Alexander 1999 but also Hardcastle and Krause 2013 for a more realistic approach) indicate that their structure is a function of time, external medium density and jet power; the first and last parameters can be linked to the source central engine. Shabala et al. (2008) find that both the radio source lifetime and duration of the quiescent phase have a strong mass de-

pendence, with massive hosts harbouring longer-lived sources that are triggered more frequently.

Indeed in the sample presented in this work, 4 to 5 sources (or 25-30% of the sample) display signs of possible restarted activity. PKS 0707-35 shows evidence for a reactivation of the jets accompanied by an axis change (Saripalli et al. 2013); PKS 2014-55, PKS 2356-61, 4C 73.08 and possibly IGR J14488-4008 are X-shaped radio galaxies that display two different lobe alignments as a result of two separate epochs of AGN activity (Saripalli and Subrahmanyam 2009, Saripalli et al. 2007, Wegowiec et al. 2016, Molina et al. 2015).

On the other hand there is now general consensus that the jet power correlates with the accretion rate and that the most powerful jets are associated to high rates of accretion (Nemmen et al. 2007, Ghisellini et al. 2014). Highly efficient accretion and large black hole mass were indeed found to characterize IGR J14488-4008 and IGR J17488-2338 (Molina et al. 2014, Molina et al. 2015) which are two recently reported GRGs selected in the soft gamma-ray band. This suggests that the most powerful and long living jets, i.e. those capable of producing Mpc radio structures as observed in GRGs, are found in AGN with exceptional internal properties, like large supermassive black holes and high rate of accretion. These are most likely the type of radio galaxies selected by current soft gamma-ray instruments like INTEGRAL/IBIS and Swift/BAT and collected here for the first time in a large sample. In this case, the lack of a correlation between radio size and soft gamma-ray luminosity (see figure 3) may simply reflect the fact that not a single parameter but a combination of parameters provides the condition for the GRGs phenomenon, with the surrounding density medium also playing a role. Indeed Malarecki et al. (2015) show the tendency for radio galaxy lobes to grow to giant sizes in directions that avoid dense regions on both small and large scales, implying that the surrounding environment is an important ingredient in the evolution of giant radio structures.

In order to better understand the reasons that lead to a much higher fraction of GRGs among soft gamma-ray selected AGN, follow up observations of the entire sample are of primary importance; first to define the subsample of GRGs in a better way and then to study the source characteristics (black hole mass, accretion rate, radio ages, detailed radio morphology, environment etc) in more details. The analysis of X/soft gamma-ray data of the entire sample has already been performed (Panessa et al. 2016) while the investigation of the radio data is well underway.

5 SUMMARY

Using recent INTEGRAL/IBIS and Swift/BAT surveys of AGN we have extracted the first sample of radio galaxies selected in the soft gamma ray band. The sample consists of 64 objects with a well defined double lobe morphology plus 3 candidate sources. The sample covers all optical classes and is dominated by HERG of the FR II type. We have measured the largest angular size of each radio galaxy and found that 60% of the objects in the sample have extensions above 0.4 Mpc and more than 20% has giant radio size (≥ 0.7 Mpc). We conclude that the fraction of GRGs among soft gamma ray selected radio galaxies is significantly larger than typically found in radio surveys, where only a few percent of objects (1-6%) have giant dimensions. This could be due to observational biases affecting the radio but not the soft gamma-ray waveband, thus preventing the detection of GRGs in radio surveys of AGN. On the contrary we do not find any evidence for selection effects

due the particular radio morphology/optical type of the objects in the sample. If the soft gamma-ray luminosity is a measure of the source power then one should expect a correlation between this parameter and the source radio size, but this is not evident in the data. This may reflect the fact that more than one parameter is involved in the production of large scale structure in radio galaxies. Our work indicates that high energy surveys represent a more efficient way to find GRGs than radio surveys.

6 ACKNOWLEDGMENTS

We acknowledge the help of 4 high school students (Nicola Borghi, Enrico Caracciolo, Matteo Rossi and Filippo Cumoli) in the analysis of the radio images; they all participated in a summer school at IASF/INAF Bologna during 2014. This project, being partly conducted by amateur astronomers under the supervision of professional scientists, represents a nice example on how citizen science work can help in dealing with a large data set. We also acknowledge ASI financial and programmatic support via contracts 2013-025-R0.

REFERENCES

- Andernach H., Jimnez Andrade E. F., Maldonado Sanchez R. F., Vsquez Baez I. R., 2012, in *Science from the Next Generation Imaging and Spectroscopic Surveys*, Published online at <http://www.eso.org/sci/meetings/2012/surveys2012/posters.html>
- Baumgartner W. H., Tueller J., Markwardt C.B. et al., 2013, *ApJS* 207, 19
- Bird A. J., Bazzano A., Bassani L. et al., 2010, *ApJS* 186, 1
- Bentjens M.A., 2011, *A&A* 526, A9
- Blundell K. M., Rawlings S., Willott C. J., 1999, *AJ* 117, 677
- Buttiglione S., Capetti A., Celotti A., 2010, *A&A* 509, 6
- Carilli C. L., Perley R. A., Harris D. E., 1994, *MNRAS* 270, 173
- Chandola Y., Saikia D.J., Gupta N., 2010, *MNRAS* 403, 269
- Condon J. J., Cotton W. D., Greisen E. W. et al., 1998, *AJ* 115, 1693
- Cotter G., Rawlings S., Saunders R., 1996, *MNRAS* 281, 1081
- Duncan R.A., Sproats L.N., 1992, *PASau* 10, 16
- Eilek J.A., 2014, *New J.Phys.*, 16, 5001
- Fanaroff B.L., Riley J.M., 1974, *MNRAS* 167, 31
- Gendre M. A., Best P. N., Wall J. V., Ker L. M., 2013, *MNRAS* 430, 3086
- Ghisellini G., Tavecchio F., Maraschi L., Celotti A., Sbarbato T., 2014, *Nature* 515, 376
- Giacintucci S., O'Sullivan E., Vrtilek J. et al., 2011, *ApJ* 732, 95
- Gopal-Krishna, Wiita P.J., 2000, *A&A* 363, 507
- Hardcastle M. J., Alexander P., Pooley G. G., Riley J. M., 1998, *MNRAS* 296, 445
- Hardcastle M. J., Evans D. A., Croston J. H., 2009, *MNRAS* 396, 1929
- Hardcastle M. J., Krause M.G.H., 2013, *MNRAS* 430, 174, 2000, *MNRAS* 319, 562
- Harwood J. J., Hardcastle M. J., Croston J. H., 2015, *MNRAS* 454, 3403
- Harris G. L. H., Rejkuba M., Harris W. E., 2010, *PASA* 27, 457
- Heckman T.M., Best P.N., 2014, *ARA&A* 52, 589
- Hocuk, S., Barthel, P. D., 2010, *A&A* 523, A9
- Hunstead R. W., Murdoch H. S., Condon J. J., Phillips M. M., 1984, *MNRAS* 207, 55
- Ishwara-Chandra C.H., Saikia D.J., 1999, *MNRAS* 309, 100
- Jamrozy M., Konar C., Saikia D. J. et al., 2007, *MNRAS* 378, 581
- Jones P. A., Lloyd B. D., McAdam W.B., 2001, *MNRAS* 325, 817
- Kaiser C. R., Alexander P., 1999, *MNRAS* 302, 515
- Koziel-Wierzbowska D., Stasinska G., 2011, *MNRAS* 415, 1013
- Krivoson R., Tsygankov S., Lutovinov A. et al., 2012, *A&A* 545, 27
- Kronberg P. P., Colgate S. A., Li H., Dufton Q. W., 2004, *ApJ*. 604, L77
- Kuzmich A., Jamrozy M., 2012, *MNRAS* 426, 851
- Landi R., Bassani L., Malizia A. et al. 2010, *MNRAS*, 403, 945

- Landt H., Bignall H.E., 2008, MNRAS 391, 967
- Landt H., Cheung C. C., Healey S. E., 2010, MNRAS 408, 1103
- Lara L., Cotton W. D., Feretti L. et al., 2001, A&A 370, 409
- Lara L., Giovannini G., Cotton W. D. et al., 2004, A&A 421, 899
- Letawe G., Courbin F., Magain P. et al., 2004, A&A 424, 455
- Lewis K. T., Eracleous M., Sambruna R. M., 2003 ApJ 593,115
- Liuzzo E., Falomo R., Treves A. et al., 2013, AJ 145, 73
- Machalski J., Jamrozy M., Zola S., 2001, A&A 371, 445
- Machalski J., Chyzy. K. T., Jamrozy M., 2004, Acta Astronomica 54, 249
- Machalski J., Jamrozy M., 2006, A&A 454,84
- Malarecki J. M., Staveley-Smith L., Saripalli L. et al., 2013, MNRAS 432, 200
- Malarecki J. M., Jones D. H., Saripalli L. et al., 2015, MNRAS 449, 955
- Malizia A., Bassani L., Bazzano A. et al., 2012, MNRAS 426, 1750
- Masetti N., Parisi P., Palazzi E. et al., 2013, A&A 556, A120
- Massardi M., Ekers Ronald D., Murphy T., 2008, MNRAS 384, 775
- Mauch T., Murphy T., Buttery H. J. et al., 2003, MNRAS 342, 1117
- Molina M., Giroletti M., Malizia A. et al., 2007, MNRAS 382, 937
- Molina M., Bassani L., Malizia A. et al., 2014, A&A 565,2
- Molina M., Venturi T., Malizia A. et al., 2015, MNRAS 451, 2370
- Mushotzky R. F., Winter L. M., McIntosh D. H., Tueller J., 2008, ApJ 684, L65
- Nemmen R. S., Bower R. G., Babul A., Storchi-Bergmann T., 2007, MNRAS 377,1652
- Nilsson K., Valtonen M. J., Kotilainen J., Jaakkola T., 1993, ApJ 413, 453
- Nilsson K., 1998 A&A 132, 31
- Panessa F., Tarchi A., Castangia P. et al., 2015, MNRAS 447,1289
- Panessa, F., Bassani L., Landi R., et al., 2016, MNRAS, submitted
- Parma P., Murgia M., Morganti R. et al., 1999, A&A 344, 7
- Pedlar A. A., Ghataure H. S., Davies R. D. et al., 1990, MNRAS 246, 477
- Reid R. I., Kronberg P. P., Perley R. A., 1999, ApJS 124, 285
- Sadler E.M., Ricci R., Ekers R. D. et al., 2006, MNRAS 371, 898
- Saripalli L., 2007, From Planets to Dark Energy: the Modern Radio Universe, Published online at SISSA, Proceedings of Science, p.130
- Saripalli L., Hunstead R. W., Subrahmanyan R., Boyce E., 2005, AJ 130, 896
- Saripalli L., Subrahmanyan R., 2009, ApJ 695, 156
- Saripalli L., 2012, AJ 144, 85
- Saripalli L., Malarecki J. M., Subrahmanyan R., 2013, MNRAS 436, 690
- Schoenmakers A. P., Mack K.H., Lara L. et al., 1998, A&A 336, 455
- Schoenmakers A. P., de Bruyn A. G., Röttgering H. J. A., van der Laan H., 2001, A&A 374, 861
- Shakura N.I., Sunyaev R. A., 1973, A&A 24, 337
- Walker R.C., Benson J. M., Unwin S.C., 1987, ApJ 316, 546
- Wezgowiec M.,Jamrozy M., Mack K. H., 2016, Acta Astron in press
- White R. L., Becker R. H., Helfand D. J., Gregg M. D., 1997, ApJ 475, 479
- Winter L. M., Lewis K. T., Koss M. et al., 2010, ApJ 710, 503
- Worrall D. M., Birkinshaw M., Young A. J. et al., 2012, MNRAS 424, 1346

Table 2. Radio Galaxies detected by *INTEGRAL*/IBIS and *Swift*/BAT

Name	z	Opt Class	Radio Morph	Log L _{IBIS} [†] erg/s	Log L _{BAT} [†] erg/s	Conv Fac kpc/arcsec	LAS _{lit} arcsec	Ref	Size _{lit} Mpc	LAS _{meas} arcsec	Size _{meas} Mpc
PKS 0018–19	0.095579	Sy1.9	FR II	-	44.6	1.784	252.0	1	0.450	280.0	0.499
PKS 0101–649	0.163000	BLQSO	FR II	-	44.9	2.821	210.0	2	0.592	220.0	0.621
3C 033	0.059700	Sy2	FR II	-	44.4	1.161	257.0	3	0.298	260.0	0.302
PKS 0131–36 (NGC612) ^d	0.029771	Sy2	FR I/II	-	44.1	0.600	852.0	4	0.511	1056.0	0.634
3C 059	0.109720	Sy1.8	FR II	-	44.7	2.015	199.0	1	0.401	200.0	0.403
3C 062	0.147000	Sy2	FR II	-	44.9	2.589	66.0	1	0.171	80.0	0.207
4C +10.08 ^b	0.070000	NLRG	FR II	-	44.2	1.345	104.0	5	0.140	160.0	0.215
B3 0309+411B ^c	0.134000	Sy1	FR II	44.9	44.9	2.395	570.0	6	1.365	480.0	1.150
LCF2001 J0318+684 (2MASX J03181899)	0.090100	Sy1.9	FR II	44.9	44.6	1.692	906.0	7	1.533	900.0	1.523
3C 84 (NGC1275) ^d	0.017559	Sy1.5	FR I	43.3	43.7	0.360	75.0	8	0.027	900.0	0.324
3C 098	0.030400	Sy2	FR II	43.9	-	0.612	310.0	3	0.190	300.0	0.184
3C 105	0.089000	Sy2	FR II	44.7	44.7	1.673	309.0	1	0.517	370.0	0.619
3C 109	0.305600	Sy1.8	FR II	-	45.6	4.551	97.0	3	0.441	105.0	0.478
3C 111	0.048500	Sy1	FR II	44.7	44.8	0.956	275.0	1	0.263	210.0	0.201
3C 120 ^e	0.033010	Sy1	FR I?	44.3	44.4	0.663	840.0	9	0.557	540.0	0.358
PKS 0442–28	0.147000	Sy2	FR II	-	45.0	2.589	86.0	1	0.223	90.0	0.233
Pic A	0.035058	Liner/Sy1	FR II	43.9	44.0	0.702	432.0	1	0.303	420.0	0.295
PKS B0521–365	0.056546	Sy1	FRI/II	44.2	44.4	1.104	60.0	10	0.066	45.0	0.050
PKS 0707–35	0.110800	Sy2	FR II	-	44.8	2.032	486.0	1	0.988	500.0	1.016
3C 184.1	0.118200	Sy2	FR II	-	44.6	2.150	182.0	3	0.391	180.0	0.387
B3 0749+460A	0.051799	Sy1.9	FR II	-	44.0	1.017	120.0	1	0.122	140.0	0.142
3C 206	0.197870	Sy1.2	FR II	-	45.4	3.298	189.0	11	0.623	205.0	0.676
4C +29.30	0.064715	Sy2	FR I/II	-	44.2	1.251	520.0	12	0.650	520.0	0.650
3C 227	0.086272	Sy1.5	FR II	-	44.6	1.627	227.0	1	0.369	230.0	0.374
4C +73.08 (VII Zw 292)	0.058100	Sy2	FR II	-	44.1	1.132	780.0	1	0.883	827.0	0.936
3C 234	0.184925	Sy1.9	FR II	-	44.9	3.125	113.0	1	0.353	115.0	0.359
PKS 1143–696	0.244000	Sey1.2	FR II	45.2	45.5	3.872	-	-	-	150.0	0.581
IGRJ13107–5626 ^f	-	-	FR II?	-11.1	-10.8	-	-	-	-	420.0	-
Centaurus A ^g	0.000880	Sey2	FR I	42.0	42.4	0.018	29520	13	0.531	25200	0.454
Centaurus B	0.012916	NLRG	FR I/II	42.8	-	0.266	1440.0	14	0.383	1600.0	0.426
3C 287.1	0.215600	Sy 1	FR II	45.2	-	3.526	117.0	1	0.413	120.0	0.423
NVSS J143649-161339 (2MASX J14364961)	0.144537	BLQSO	FR I/II	-	45.0	2.553	720.0	15	1.838	714.0	1.823
IGR 14488–4008	0.123000	Sy1.2	FR II	44.3	44.7	2.225	692.0	16	1.540	692.0	1.540
3C 309.1	0.905000	Sy1.5	C	-	46.6	7.910	2.1	1	0.017	2.0	0.016
4C +63.22	0.204000	Sy1	FR II	-	45.0	3.377	210.0	6	0.709	210.0	0.709
3C 323.1	0.264300	Sy1.2	FR II	-	45.2	4.107	70.4	1	0.289	100.0	0.411
4C +23.42	0.118000	Sy1	FR I	-	44.6	2.147	-	-	-	150.0	0.322
S5 1616+85 (Leda 100168)	0.183000	Sy1	FR II	-	45.1	3.099	87.0	1	0.270	140.0	0.434
3C 332	0.151019	Sy1	FR II	-	45.2	2.648	73.0	1	0.193	100.0	0.265
WN 1626+5153 (Mrk 1498)	0.054700	Sy1.9	FR II	-	44.5	1.070	1140.0	5	1.220	1125.0	1.204
4C +34.47	0.206000	Sy1	FR II	-	45.4	3.403	259.0	17	0.881	240.0	0.817
PKS 1737–60	0.410000Phot	-	FR II	-	45.8	5.507	78.0	1	0.430	90.0	0.496

Soft γ -ray selected radio galaxies: favouring giant size discovery

Table 3. continued

Name [†]	z	Opt Class	Radio Morph	Log L _{IBIS} [‡] erg/s	Log L _{BAT} [‡] erg/s	Conv Fac kpc/arcsec	LAS _{lit} arcsec	Ref	Size _{lit} Mpc	LAS _{meas} arcsec	Size _{meas} Mpc
4C +18.51	0.186000	Sy1	FR II	-	45.1	3.140	212.0	1	0.666	220.0	0.691
IGR J17488–2338	0.240000	Sy1.5	FR II	45.2	-	3.825	370.0	18	1.415	370.0	1.415
3C 380	0.692000	Sy1.5	FR II	-	46.6	7.199	7.5	19	0.054	15.0	0.108
3C 382	0.057870	Sy1	FR II	44.5	44.8	1.129	186.0	3	0.210	180.0	0.203
3C 390.3	0.056100	Sy1.5	FR II	44.6	44.9	1.096	229.0	3	0.251	230.0	0.252
PKS 1916–300 ^g	0.166819	Sy1.5/1.8	FR II	44.8	45.1	2.875	45.0	20	0.129	150.0	0.431
3C 403	0.059000	Sy2	FR II	44.2	44.5	1.149	97.0	1	0.111	250.0	0.287
Cygnus A	0.056075	Sy1.9	FR II	44.8	45.0	1.095	122.0	21	0.136	115.0	0.126
PKS 2014–55	0.060629	Sy2	FR I	-	44.5	1.178	1284.0	22	1.513	1260.0	1.484
4C +21.55	0.173500	Sy1	FR II	45.1	45.4	2.969	-	-	-	192.0	0.570
4C +74.26	0.104000	Sy1	FR II	45.0	45.2	1.922	610.0	5	1.172	630.0	1.211
S5 2116+81(2MASX J21140128)	0.084000	Sy1	FR I	44.7	44.8	1.589	360.0	6	0.572	340.0	0.540
4C 50.55	0.020000	Sy1	FR II	44.0	44.3	0.408	570.0	23	0.233	468.0	0.191
3C 433	0.101600	Sy2	FR I/II	-	44.6	1.883	69.0	3	0.130	45.0	0.085
PKS 2135–14	0.200470	Sy1.5	FR II	-	45.2	3.332	160.0	1	0.533	150.0	0.500
PKS 2153–69	0.028273	Sy1	FR II	-	43.4	0.571	60.0	24	0.034	80.0	0.046
MG3 J221950+2613 (2MASX J22194971)	0.085000	Sy1	FR II	-	44.5	1.606	-	-	-	200.0	0.321
3C 445	0.055879	Sy1.5	FR II	-	44.5	1.092	570.0	25	0.622	600.0	0.655
3C 452	0.081100	Sy2	FR II	44.6	44.7	1.539	278.0	3	0.428	280.0	0.431
PKS 2300–18	0.128929	Sy1	FR II?	-	44.6	2.317	280	26	0.649	270.0	0.626
PKS 2331–240	0.047700	Sy2	FR II	-	43.9	0.941	1260	27	1.186	1248.0	1.174
PKS 2356–61	0.096306	Sy2	FR II	-	44.5	1.796	410	22	0.736	400.0	0.718
candidates											
PKS 0921–213	0.052000	Sy1		-	44.0	1.021				1050.0	1.072
IGR J18249–3243	0.355000	Sy1		45.4	-	5.032				100.0	0.503
2MASX J23272195+1524375	0.045717	Sy1		-	43.7	0.904				1020.0	0.922

[†] We have used the radio source name; the name used in the soft gamma-ray surveys is reported in parenthesis if not coincident with the radio one;

[‡] IBIS luminosity in the 20–100 keV band. BAT Luminosity in the 14–195 keV band; note that the luminosity of NGC 1275 could be contaminated by the Perseus cluster; similarly is the case of CenB where the INTEGRAL luminosity could be contaminated by the nearby AGN 4U 1344–60;

Notes: a) Our LAS measurement takes into account the northern extension of the western lobe, which explains the difference with the value reported in the literature; b) Our LAS measurement takes into account the two tails visible on the NVSS image; c) the difference in source size is irrelevant in this case given that both measurements provide a size well above the threshold for GRGs definition; d) This radio galaxy is located at the centre of the Perseus cluster and is surrounded by the well-known mini-halo (e.g. Bentjens 2011); our measurement refers to the current activity of the AGN; e) The morphology of this source is very complex; our measurement refers to the largest extension (in the N-S direction) visible on NVSS; f) This source is detected at the reported flux (log F in units of erg cm⁻² s⁻¹) but we are unable to estimate the Luminosity without a knowledge of the source redshift; g) For Cen A we have adopted the redshift corresponding to the latest distance estimate of 3.8 Mpc (Harris et al. 2010); h) The source dimension quoted in the literature for this source comes from a very old radio map while our estimate is based on the NVSS image.

References: 1) Nilsson 1998; 2) Sadler et al. 2006; 3) Leahy, Bridle & Strom in <http://www.jb.man.ac.uk/atlas/>; 4) Gopal-Krishna and Wiita 2000; 5) Landt and Bignall 2008; 6) Ishwara-Chandra & Saikia 1999; 7) Lara et al 2001; 8) Pedlar et al. 1990; 9) Walker, Benson & Unwin 1987; 10) Liuzzo et al. (2013); 11) Reid, Kronberg and Perley 1999; 12) Jamroz et al. 2007; 13) Eilek 2014; 14) Jones et al. 2001; 15) Letawe et al. 2004; 16) Molina et al. 2015; 17) Hocuk & Barthel (2010); 18) Molina et al 2014; 19) Nilsson et al 1993; 20) Duncan and Sproats 1992; 21) Carilli et al. 1994; 22) Saripalli and Subrahmanyam 2009; 23) Molina et al. 2007; 24) Worrall et al. 2012; 25) Hardcastle et al. 1998; 26) Hunstead et al. 1984; 27) Massardi et al. 2008.